A&A 472, 537–545 (2007)
DOI: 10.1051/0004-6361:20077358

Astronomy & Astrophysics

The CH_2CN^- molecule: carrier of the λ8037 diffuse interstellar band?

M. A. Cordiner[1,2] and P. J. Sarre[1]

[1] School of Chemistry, The University of Nottingham, University Park, Nottingham NG7 2RD, UK
e-mail: m.cordiner@qub.ac.uk
[2] Astrophysics Research Centre, School of Mathematics and Physics, Queen's University, Belfast BT7 1NN, UK

Received 23 February 2007 / Accepted 4 July 2007

ABSTRACT

The hypothesis that the cyanomethyl anion CH_2CN^- is responsible for the relatively narrow diffuse interstellar band (DIB) at 8037.8 ± 0.15 Å is examined with reference to new observational data. The 0_0^0 absorption band arising from the $^1B_1 - \tilde{X}\ ^1A'$ transition from the electronic ground state to the first dipole-bound state of the anion is calculated for a rotational temperature of 2.7 K using literature spectroscopic parameters and results in a rotational contour with a peak wavelength of 8037.78 Å. By comparison with diffuse band and atomic line absorption spectra of eight heavily-reddened Galactic sightlines, CH_2CN^- is found to be a plausible carrier of the λ8037 diffuse interstellar band provided the rotational contour is Doppler-broadened with a b parameter between 16 and 33 km s^{-1} that depends on the specific sightline. Convolution of the calculated CH_2CN^- transitions with the optical depth profile of interstellar Ti II results in a good match with the profile of the narrow λ8037 DIB observed towards HD 183143, HD 168112 and Cyg OB2 8a. The rotational level populations may be influenced by nuclear spin statistics, resulting in the appearance of additional transitions from $K_a = 1$ of ortho CH_2CN^- near 8025 and 8050 Å that are not seen in currently available interstellar spectra. For CH_2CN^- to be the carrier of the λ8037 diffuse interstellar band, either a) there must be mechanisms that convert CH_2CN^- from the ortho to the para form, or b) the chemistry that forms CH_2CN^- must result in a population of K_a'' levels approaching a Boltzmann distribution near 3 K.

Key words. astrochemistry – ISM: lines and bands – ISM: molecules – ISM: atoms – ISM: clouds

1. Introduction

The origin of the unidentified diffuse interstellar bands (DIBs) remains one of the greatest challenges in astronomical spectroscopy. The subject has been reviewed by Herbig (1995) and Sarre (2006) who have highlighted research that points towards organic molecules as likely candidates for at least some of the more than 300 DIBs. Sarre (2000) has put forward a hypothesis that "some, possibly many" of the diffuse interstellar bands arise from electronic transitions between ground and dipole-bound states of negatively charged polar molecules or small polar grains. It was noted that the $^rQ_0(1)$ line of the origin band of the $^1B_1 - \tilde{X}\ ^1A'$ transition of CH_2CN^- occurs at 8037.8 Å, in good correspondence with the peak absorption wavelength of a diffuse interstellar band at 8037.9 ± 0.3 Å (Galazutdinov et al. 2000).

2. Molecular anions as diffuse band carriers

2.1. Previous studies

The electronic absorption spectrum of C_7^- in the visible region was studied by Tulej et al. (1998) and five optical absorption bands were reported to match with the wavelengths of known DIBs. Models of diffuse cloud chemistry by Ruffle et al. (1999) that incorporated the desorption of seed molecules from grain surfaces were able to reproduce large abundances of C_7^- (approximately $10^{-9} n_H$), and also of C_7H^-, albeit only under a limited set of physical and chemical conditions and only for short periods of time. The high electron affinity and density of vibrational states of C_7 permits rapid radiative electron attachment such that anion formation has been calculated to occur every time an electron collides with C_7 (Terzieva & Herbst 2000). However, the early promise of C_7^- as a DIB carrier was quashed when high resolution observational and laboratory spectroscopy by Galazutdinov et al. (1999), Sarre & Kendall (2000), Lakin et al. (2000) and McCall et al. (2001) identified that the match between the DIBs and the wavelengths, strengths and profiles of the C_7^- optical absorption bands was too poor to constitute an assignment.

Based on laboratory spectroscopy it was suggested by Güthe et al. (2001) that CH_2CC^- might be a diffuse band carrier but a detailed assessment by McCall et al. (2002b) showed that the wavelength match to the diffuse band at 6993 Å was not acceptable and commented that the non-observation of additional K sub-bands argued against an assignment to CH_2CC^-. The CH_2CN^- molecule has many spectroscopic characteristics in common with CH_2CC^-, both molecules being near-prolate asymmetric tops with ortho and para forms and both possessing dipole-bound excited states, but CH_2CN^- has a closed electronic shell.

2.2. Anion chemistry in the ISM

Chemistry in the diffuse ISM (with kinetic temperatures of ~50 K, densities ~100 cm^{-3} and strong UV radiation fields) has been shown to be rich and complex by observations which include the detection of polyatomic molecules such as H_3^+ (McCall et al. 1998), C_3 (Maier et al. 2001), and HCO^+, HCN, H_2CO, C_2H and c-C_3H_2 (Lucas & Liszt 1996a,b, 2000;

Liszt & Lucas 2001) at high fractional abundances similar to those observed in dark clouds. Conventional models of gas-phase diffuse cloud chemistry struggle to explain how such high molecular abundances can be maintained in the interstellar UV radiation field. However, as discussed by Duley & Williams (1984) and Hall & Williams (1995), the availability of erosion products from carbonaceous dust grains, including polyynes (C_n chains) and small molecules such as diacetylene (C_4H_2), could provide a reservoir of reagents to fuel a complex network of organic reactions in diffuse clouds and other photon-dominated regions. Large molecules should be able to resist photodissociation in the interstellar UV field by undergoing internal conversion in which the energy of absorbed photons is redistributed into the vibrational modes of the molecule due to the high density of states. To date the role of anions in interstellar reaction networks has generally been considered to be minimal although some consideration of their possible detection in the interstellar medium has been made (Sarre 1980). No reaction pathways involving anions were present in the "comprehensive" diffuse cloud models of van Dishoeck & Black (1986) (where ~500 reactions were modelled), and only a few atomic and diatomic anions are present in the UMIST 1999 database of ~4000 astrochemical reactions involving ~400 different species (Le Teuff et al. 2000). This is at least partly due to the lack of observational evidence for anions in space, but also reflects a common view that anions should be rapidly photoionised in the interstellar UV field.

The abundance of interstellar anions in relatively diffuse media depends in large part on the balance between radiative electron attachment (Dalgarno & McCray 1973) and photodetachment by the interstellar radiation field. As discussed by Herbst (1981) and Herbst & Petrie (1997), a viable route for molecular anion formation in the ISM involves attachment of a free electron via the formation of an excited temporary anion that stabilises through radiative transitions to the ground state. Provided the radiative transition rate is high, anions should be able to form at a sufficient rate that – relative to their neutral counterparts – appreciable anion abundances may occur depending on the local interstellar gas pressure and radiation field. Chemical models of the circumstellar envelope of the carbon star IRC+10°216 by Millar et al. (2000) predict observable abundances of C_n^-, C_nH^- and C_nN^-. The discovery of the microwave signature of C_6H^- in IRC+10°216 and TMC-1 by McCarthy et al. (2006) at fractional abundances (relative to the neutral species C_6H) of about 2.5% and 1%, respectively, proves that anions arise in some regions of space in significant quantities.

2.3. Dipole-bound states

Anions derived from strongly polar neutral parent molecules (or grains) can support one or more "dipole-bound" electronic states at energies near to the detachment threshold and can potentially form the excited states in electronic absorption spectra in the visible region of the spectrum. Dipole-bound electronic states were first predicted by Fermi & Teller (1947) who showed that a theoretical point dipole with a sufficiently large dipole moment (>1.625 D) can bind an electron in a diffuse orbital. Theoretical studies (Crawford 1970; Garrett 1978; Gutsev & Adamowicz 1995a,b,c) and experimental work (Moran et al. 1987; Brinkman et al. 1995; Lykke et al. 1987; Desfrançois et al. 1996) has since demonstrated that in practice, dipole moments $\mu \gtrsim 2.5$ D are required for a molecule to support at least one dipole-bound electronic state. Laboratory studies of nitromethane (Compton et al. 1996) and of cyanoacetylene and uracil (Sommerfeld 2005) indicate that the presence of a near-threshold dipole-bound state can act as a "doorway" for electron capture, and that strong electronic transitions occur from the dipole-bound state to the ground state, resulting in rapid radiative stabilisation of the anion. It is possible that this effect may enhance the electron capture rate for the strongly dipolar C_6H molecule and therefore contribute towards the abundance of C_6H^- observed by McCarthy et al. (2006).

Table 1. Table showing sightline data for λ8037 observations. For the E_{B-V} values, $B - V$ photometry are from Perryman & ESA (1997) and spectral types from the modal averages of all data referenced in the SIMBAD database (URL: `http://simbad.u-strasbg.fr/sim-fid.pl`); intrinsic stellar photometry is from Wegner (1994) with the exception of Cyg OB2 5 and 8a for which photometry was taken from Massey & Thompson (1991) and Cyg OB2 12 which is of uncertain spectral type and photometry as discussed by Gredel & Munch (1994). Approximate stellar distances d (accurate to around ±50%), were calculated from the spectral types and absolute magnitudes of Wegner (2006) (stellar apparent magnitudes were dereddened assuming a ratio of visual to selective extinction (R_V) of 3.1).

Target	Sp. type	V	E_{B-V}	d (pc)
Cyg OB2 5	O7 Ie	9.2	1.94	700
Cyg OB2 8a	O6 I	9.0	1.59	1000
Cyg OB2 12	B2 I–B8 Ia	11.4	2.8–3.4	600
HD 168112	O5	8.6	1.01	2000
HD 169034	B5 Ia	8.2	1.3	1100
HD 183143	B7 Ia	6.9	1.24	650
HD 186745	B8 Ia	7.1	0.96	1600
HD 229196	O5	8.6	1.22	1100
λ Cyg	B5 V	4.6	0.04	50
ζ Peg	B8.5 V	3.4	0.00	50

3. Spectroscopic observations and data reduction

Medium resolution optical spectroscopic observations of early-type Galactic stars were performed using the High Resolution Echelle Spectrograph (HIRES) of the W. M. Keck Observatory, Hawaii by G. H. Herbig between 1995 and 1997 (private communication), who kindly made available the raw science exposures of eight heavily-reddened Galactic sightlines (shown in Table 1), including flat fields, Th/Ar and bias frames. Reductions were carried out using standard **IRAF** echelle routines. In the region of the λ8037 DIB special care was taken to eliminate telluric lines and fringing residuals by division with high S/N standard star spectra. The S/N of the reduced spectra is typically between 400 and 800 per pixel, with a resolving power of 42 500 (measured from the average of several unblended Th/Ar lines over the wavelength range of ~7000 to 10 000 Å). In addition, near-UV spectra from ~3200 to 4000 Å were obtained for the sight-lines towards Cyg OB2 8a, HD 168112 and HD 183143 and include spectra of a range of important interstellar species including Ca II, Ti II and various diatomic molecules that provide valuable information on the velocity distribution of the interstellar gases. The near-UV spectra typically have $S/N \sim 300$ with a resolving power of 52 500. Around 8040 Å the wavelength drift between successive arcs was 0.02 Å, and for the near-UV observations (around 3600 Å) the drift was 0.005 Å. Thus, absolute wavelength calibration errors should be $\Delta\lambda/\lambda \lesssim 2.5 \times 10^{-6}$ (0.75 km s^{-1}) for the red/NIR and $\lesssim 1.4 \times 10^{-6}$ (0.4 km s^{-1}) for the near-UV spectra.

4. Spectroscopy of CH_2CN^-

The neutral cyanomethyl radical CH_2CN has a dipole moment between *c.* 3.5 and 4.0 D (Ozeki et al. 2004) and an electron affinity of *c.* 1.55 eV (Lykke et al. 1987). The first dipole-bound state of the *anion* lies ≃10 meV below the ionisation continuum (Lykke et al. 1987; Moran et al. 1987; Gutsev & Adamowicz 1995a). The CH_2CN radical is planar but on attachment of an electron the hydrogen atoms move out of plane, resulting in a $\tilde{X}\ ^1A'$ electronic ground state in C_s symmetry (Gutsev & Adamowicz 1995a) with the mirror plane along the C-C-N backbone. In the excited $^1B_1$ state, the dipole-bound electron is very diffuse with only a weakly perturbative interaction with the rest of the molecule. Thus in the dipole-bound state the nuclear framework assumes a geometry which is almost identical to that of the ground-state neutral radical. The $^1B_1 - \tilde{X}\ ^1A'$ transition is of perpendicular type (Lykke et al. 1987) with the transition dipole orientated along the *c*-axis and selection rules $\Delta J = \pm 1$, $\Delta K_a = \pm 1$ (K_a is used although it is not strictly a good quantum number). The rotational constants of CH_2CN^- were determined to very high accuracy by Lykke et al. (1987) using high-resolution fast-ion-beam autodetachment spectroscopy. The rotational energy level structure and some examples of $^1B_1 - \tilde{X}\ ^1A'$ transitions are shown in Fig. 4. of Lykke et al. (1987).

Nuclear spin statistics dictate that there exist ortho (*o*) and para (*p*) forms of CH_2CN^- as occurs in the isoelectronic molecule cyanamide (NH_2CN), discussed by Millen et al. (1962). If the ortho and para CH_2CN^- abundances reflect the *o*:*p* (3:1) nuclear spin degeneracies, transitions of ortho CH_2CN^- would be three times stronger than equivalent transitions of the para form. It not clear whether thermalisation of the rotational energy levels of CH_2CN^- would take place, but based on observations of other interstellar molecules, it is evident that ortho-to-para abundance ratios do not necessarily follow the nuclear spin degeneracies. For example, according to Flower & Watt (1984), interconversion between ortho and para H_2 occurs via collisional proton exchange in the reaction $o\text{-}H_2 + H^+ \longrightarrow p\text{-}H_2 + H^+ + h\nu$, which allows the population of the lowest J levels to reach thermal equilibrium with the ISM such that *o*:*p* is skewed away from the value of 3:1. In the case of CH_2CN^- the photodetachment (destruction) rate has been calculated to be approximately 1.2×10^{-8} s^{-1} (E. Herbst & T. J. Millar, private communication); given the relatively slow rate of conversion between gas-phase ortho and para H_2 by proton exchange with H^+ ($3 \times 10^{-10} n_{H^+}$ s^{-1}; Flower & Watt 1984), it follows that in the neutral ISM where H^+ densities are generally less than 0.1 cm^{-3}, collisional exchange with gas-phase CH_2CN^- is unlikely to alter significantly the ortho-to-para population ratio.

For molecules with equivalent H atoms the rotational level populations (and *o*:*p* ratios) can give clues as to the chemical reactions in which the molecule participates. For example, if a molecule is formed by reaction with H_2, then the *o*:*p* ratio of the product may be influenced by the *o*:*p* ratio of the reagent H_2 (see the case of *c*-C_3H_2, studied by Takakuwa et al. 2001). Also, according to Dickens & Irvine (1999), the observed *o*:*p* ratio of H_2CO, (which has the same nuclear spin statistical properties as CH_2CN^-), indicates that the molecules probably formed in thermal equilibrium with cold dust grains. Both of these types of reactions could potentially influence the *o*:*p* ratio of CH_2CN^-.

5. Results

Using the molecular constants of Lykke et al. (1987) and the ASYROT FORTRAN code (Birss & Ramsay 1984), the $^1B_1 - \tilde{X}\ ^1A'$ transitions of CH_2CN^- were computed for a distribution of rotational level populations in equilibrium with the 2.74 K CMB. Isoelectronic with NH_2CN (dipole moment 4.32 D; Tyler et al. 1972), the cyanomethyl anion is expected to have a large dipole moment (∼4 D) such that in the diffuse ISM the radiative transition rate is sufficient that collisional excitation of the molecule should be small. Small changes in the level of (J) rotational excitation of the molecule in fact have relatively little impact on the spectrum, which is dominated by the Q branch of the transition at 8037.8 Å. Convolved with a Gaussian with Doppler $b = 1$ km s^{-1} and at a resolving power of 42 500, the calculated spectrum is displayed in Fig. 1 for comparison with the observed HIRES spectra.

Examination of the spectrum of the standard star λ Cyg shows no evidence for significant stellar lines, fringing artifacts or telluric residuals across the wavelength region. The most prominent features are the λ8026 DIB, which is among the narrowest known diffuse bands, and an absorption feature around 8037 Å. The λ8037 DIB is relatively narrow (*FWHM* ∼ 1.3−2 Å), but is overlapped by a broader absorption centered at around 8040 Å (noted by Herbig & Leka 1991) that is most prominent towards Cyg OB2 12 and HD 183143. The λ8040 component has a *FWHM* of around 4 Å and forms an absorption peak at 8040.7 ± 0.3 Å. In the co-added (K I rest frame) spectra (shown in Fig. 2), Gaussian fits to the peak of the λ8037 DIB give a wavelength of 8037.8 ± 0.15 Å for this diffuse interstellar band.

The peak wavelength match of λ8037 with the 2.7 K $^1B_1 - \tilde{X}\ ^1A'$ CH_2CN^- spectrum shown in Fig. 1 is very good. However, the computed spectrum clearly contains significant fine structure that is not present in any of the observed λ8037 profiles. The Q branch of the $K_a'' = 0$ transition creates the prominent peak at 8037.78 Å. The P branch is of rather low intensity compared to the R branch that produces the set of lines between 8035 and 8037.2 Å. Evidence for asymmetry of λ8037 can be seen in the blue degradation of the DIB spectra for the three Cyg OB2 sightlines and HD 183143, HD 186745 and HD 229196. The band shows significant evidence for profile variability across all of the sightlines, especially in comparing HD 186745 and HD 183143 with Cyg OB2.

The variable strength and profile of λ8040 with respect to λ8037 suggests that it is probably caused by a different carrier. Towards Cyg OB2 5 and HD 168112, the λ8040 DIB has *FWHM* ∼ 11.5 Å – much broader than in the other sightlines – and perhaps indicates the presence of *another* broad DIB. To isolate the λ8037 DIB for analysis is non-trivial among these other contaminating features. However, it is relatively narrow which assists its rejection in continuum fitting algorithms such that consistently repeatable continuum fits were possible.

5.1. Ortho and para CH_2CN^-

As detailed in Sect. 4, CH_2CN^- is expected to exist in the ISM in para and ortho forms, with the lowest occupied rotational levels being $J'' = 0$, $K_a'' = 0$ and $J'' = 1$, $K_a'' = 1$, respectively. The $K_a = 1 \longleftarrow 0$ transitions peak around 8037.8 Å, whereas the $K_a = 0 \longleftarrow 1$ and the $K_a = 2 \longleftarrow 1$ transitions peak at 8049.6 and 8024.8 Å respectively. The λ8037 co-added spectrum for all eight sightlines is plotted in Fig. 2 with para + ortho CH_2CN^- $^1B_1 - \tilde{X}\ ^1A'$ transitions, convolved with a rest cloud model ($v_{LSR} = 0$ km s^{-1}) with Doppler $b = 18$ km s^{-1} and an arbitrary intensity scaling. Two K_a'' population scenarios are

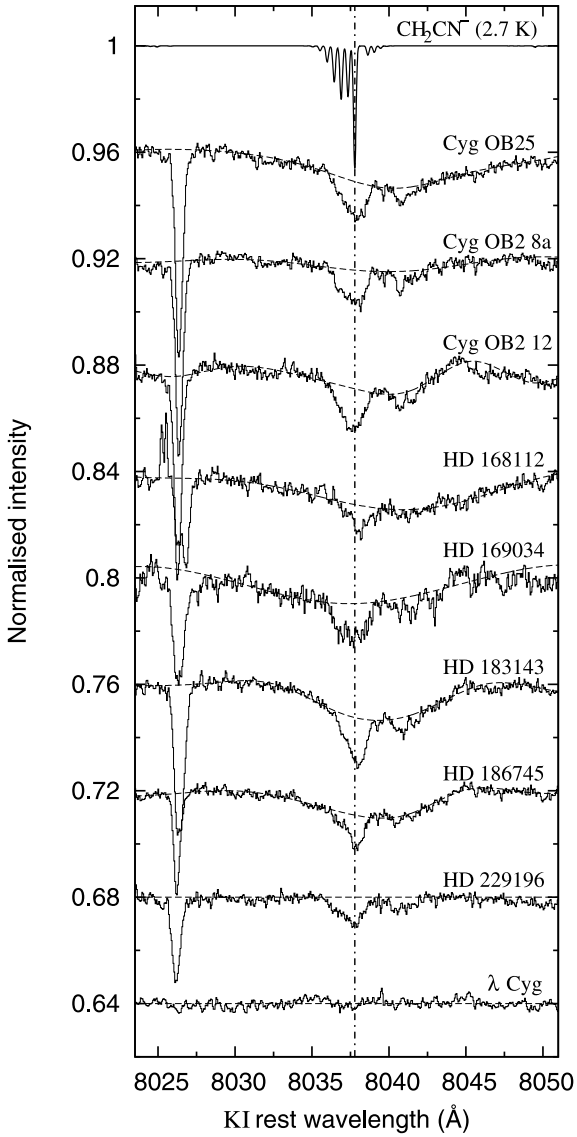

Fig. 1. Normalised (second order Chebyshev polynomial), telluric-corrected HIRES spectra of the region around 8037 Å. Spectra have been Doppler shifted to place the mean K I wavelength at rest (using $\lambda_{\mathrm{K\,I\ rest}}$ = 7698.9645 Å (Morton 2003). λ Cyg is shown as an unreddened standard. Fitted continua are shown as dashed lines. The 2.74 K CH_2CN^- $^1B_1 - \tilde{X}\ ^1A'$ origin band absorption spectrum is plotted at the top, calculated assuming a single cloud at rest with Doppler b = 1 km s^{-1} and convolved to the resolving power R = 42 500 of the HIRES spectra. The K_a'' = 0 transitions lie between 8035 and 8040 Å and at this temperature the K_a'' = 1 transitions at around 8025 and 8046 Å are almost invisibly weak. The absorption feature at around 8026 Å is an unrelated diffuse interstellar band.

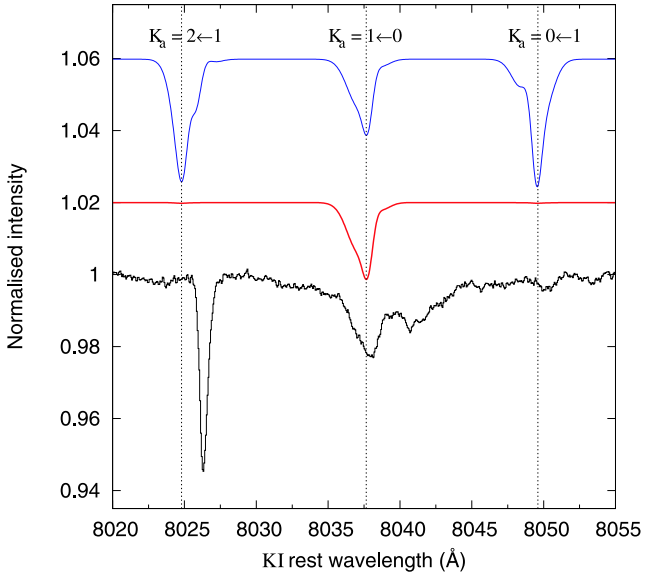

Fig. 2. Comparison of computed and observed (averaged) spectra in the 8037 A region. The bottom trace shows the *co-added*, normalised, telluric-corrected HIRES spectrum around λ8037 observed towards the stars listed in Table 1. Spectra were Doppler-shifted to place the weighted-mean K I wavelength at rest before co-addition. The $^1B_1 - \tilde{X}\ ^1A'$, $\{K_a = 2 \longleftarrow 1, K_a = 1 \longleftarrow 0, K_a = 0 \longleftarrow 1\}$ modelled absorption spectrum is shown, and includes the transitions arising from both $K_a'' = 0$ (para) and $K_a'' = 1$ (ortho) CH_2CN^-. The middle spectrum was calculated assuming a thermal Boltzmann distribution of K_a level populations. The upper spectrum shows the result taking the K_a'' populations to be determined solely by a 3:1 nuclear spin-statistical weight ortho:para ratio for odd:even K_a'' levels. The interstellar CH_2CN^- distribution is modelled as a single cloud at rest (v = 0 km s^{-1}) with Gaussian line-shape (Doppler b = 18 km s^{-1}), convolved to the resolving power R = 42 500 of the HIRES spectra. The respective peak absorption wavelengths of the three Doppler-broadened K_a sub-bands are 8024.8, 8037.7, and 8049.6 Å, shown as dotted lines and correspond to ortho, para and ortho CH_2CN^- respectively.

plotted: (1) a 3:1 ratio of odd: even K_a'' level populations and (2) a 2.74 K Boltzmann distribution.

The predicted $K_a = 2 \longleftarrow 1$ transitions (with peak absorption at ~8024.8 Å) partially overlap the narrow λ8026 DIB. There is some evidence for a small blue shoulder on this DIB, at a wavelength slightly blue of the peak CH_2CN^- $K_a = 2 \longleftarrow 1$ absorption wavelength. The $K_a = 0 \longleftarrow 1$ feature (with peak absorption at ~8049.6 Å) falls close to a small absorption feature in the co-added spectrum. In this spectrum, the central depth of the λ8037 feature is 1.35±0.16% and the central depth of the λ8049 feature is 0.3 ± 0.16% (2σ error estimates derived from the rms noise of the continuum). The ratio of the central depth of the λ8037 to λ8049 features is consistent with a *o*:*p* ratio of ~1:2.3, but given the mismatch between the calculated and observed profile and peak wavelength, it seems unlikely that λ8049 is caused by *o*-CH_2CN^-.

From Fig. 2, it is clear that if interstellar CH_2CN^- has a 3:1 "statistical" ratio of *o*:*p* states, it cannot be the carrier of the λ8037 DIB due to the lack of the ortho transitions at the expected strengths in the observed spectra. The λ8026 DIB is too red relative to the *Q* branch (main peak) of the $K_a = 2 \longleftarrow 1$ transition to constitute a spectroscopic match with the model calculation. If however the K_a level populations have, or approach, a Boltzmann distribution, then the transitions originating in $K_a = 1$ are sufficiently weak for CH_2CN^- to be a plausible carrier of the λ8037 diffuse interstellar band.

5.2. Modelling the λ8037 diffuse interstellar band

As shown by Figs. 1 and 2, a large Doppler broadening of the interstellar gas is required for CH_2CN^- to be the carrier of λ8037. Based on the assumption that the λ8037 DIB is caused by the origin band $^1B_1 - \tilde{X}\ ^1A'$, $K_a'' = 0$ transitions of CH_2CN^- at 2.74 K, it is possible to use the shape of the DIB to infer the shape of the hypothetical interstellar CH_2CN^- velocity distribution. This distribution may then be compared with observed interstellar

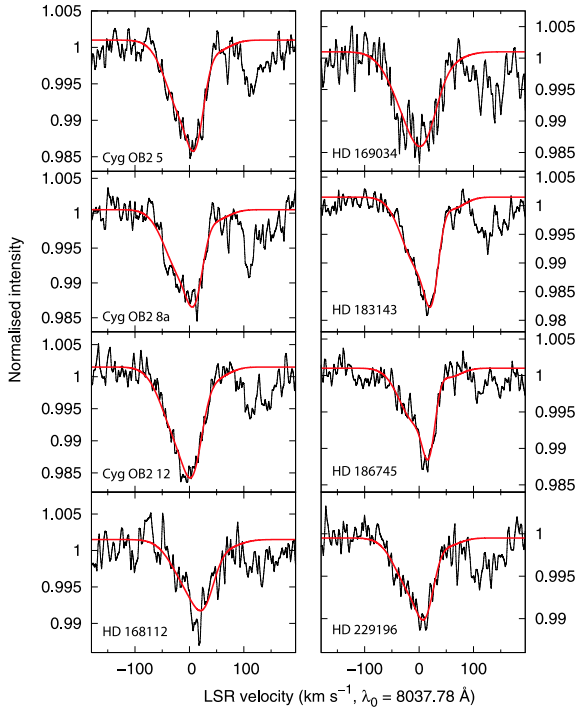

Fig. 3. Telluric-corrected, normalised DIB λ8037 spectra (thin black traces) and least-squares fitted CH_2CN^- $^1B_1 - \tilde{X}\ ^1A'$, $K_a = 1 \longleftarrow 0$ models (thick red traces). Models employ a single Gaussian interstellar cloud. Radial velocity shift, Doppler width, central depth and an additive continuum offset were free parameters in the fits. The DIB rest wavelength was set at $\lambda_0 = 8037.78$ Å for the displayed velocity scale. Best-fitting model parameters are shown in Table 2 and the inferred CH_2CN^- interstellar velocity distributions plotted in Fig. 4 (lines labeled "Mdl").

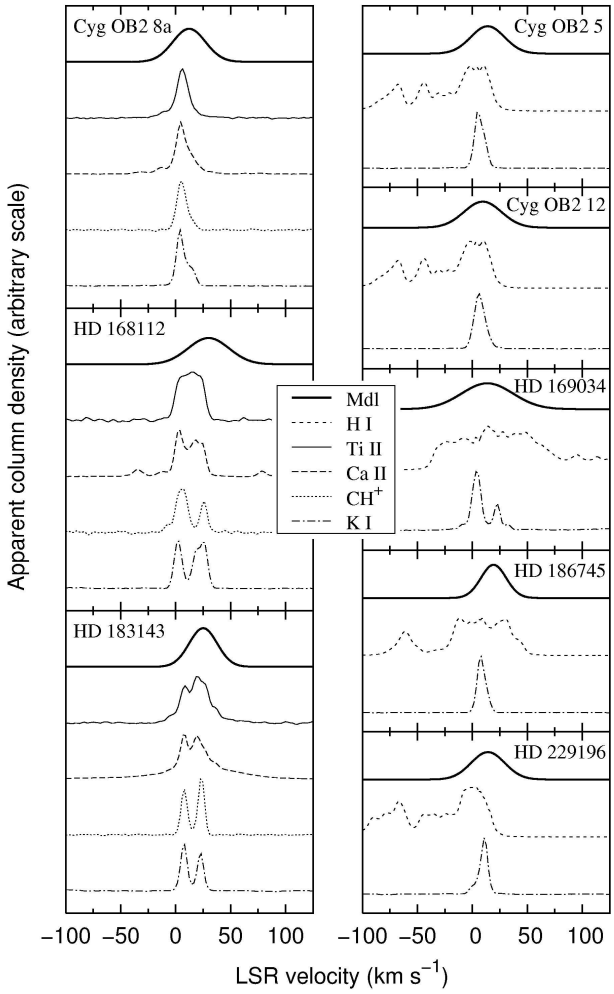

Fig. 4. Each of the eight panels above shows LSR velocity-space apparent column density profiles for interstellar species for which data were available. Data for the K I 7699 Å, CH^+ 3958 Å, Ca II 3968 Å and Ti II 3384 Å lines are shown. Hypothetical model CH_2CN^- velocity distributions (labeled "Mdl") are shown at the top of each panel, calculated based on the fits shown in Fig. 3 (parameters given in Table 2) with the assumption that the narrow λ8037 DIB is caused by the origin band $^1B_1 - \tilde{X}\ ^1A'$ transitions of CH_2CN^- at 2.74 K, and that the interstellar velocity distribution of the gas is Gaussian. The interstellar K I, CH^+, Ca II and Ti II apparent column densities (N_a) were calculated from the normalised HIRES spectra (I/I_0, where I_0 is the continuum intensity) according to $N_a \propto \ln(I_0/I)$ (see for example Savage & Sembach 1991). For the right-hand panel, H I column density profiles are from the Leiden/Argentine/Bonn (LAB) Survey of Galactic H I (Kalberla et al. 2005).

velocity profiles for different species in the observed sightlines. The computed 2.74 K absorption spectrum was subjected to a least-squares analysis whereby it was convolved with a single Gaussian interstellar cloud model with the Doppler width, mean radial velocity and equivalent width floated as free parameters. A fourth free parameter allowed an additive shift in the continuum height if necessary. The least-squares parameters for each sightline are shown in Table 2, and the corresponding DIB model spectrum and CH_2CN^- velocity distribution are shown in Figs. 3 and 4, respectively. The quality of the fits was monitored by comparing the normalised continuum rms of the observed spectra (σ_c) with the normalised rms of the model fit residuals (σ_f).

5.3. Hypothetical interstellar CH_2CN^- distribution

As shown by Fig. 3, the model fits match the spectra to a high degree of accuracy for each of the eight sightlines. Variations in the width and structure of the DIB profile can be reproduced in each case, highlighted by the progression of the λ8037 *FWHM* from narrow to wide in the sequence HD 186745 → HD 183143 → Cyg OB2 12 → HD 169034. The progression corresponds to a sequential increase in the Doppler *b* of the cloud model: 16.2 → 18.0 → 24.0 → 33.0 km s^{-1}. Such large *b* values would require unphysically large kinetic and/or turbulent gas velocities and clearly cannot arise in a single interstellar cloud, and this places some doubt on the validity of the single-cloud model used here. However, given the S/N of the spectra, there is no statistical justification for employing more than one cloud in the model. The Gaussian cloud model fits the DIB well as shown by $\sigma_c \approx \sigma_f$, implying that if CH_2CN^- is the λ8037 carrier, its interstellar velocity distribution must be approximately Gaussian.

Comparing the hypothetical CH_2CN^- velocity structures with the profiles of interstellar lines in Fig. 4 shows that the calculated CH_2CN^- distributions are reasonably close to the velocities of the diffuse interstellar clouds. Due to the lack of spectroscopic data for other interstellar species for five of the sightlines examined, H I data were obtained from the Leiden/Argentine/Bonn (LAB) survey (Kalberla et al. 2005, data available at `http://www.astro.uni-bonn.de/~webrai/english/tools_labsurvey.php`). Although background H I emission contaminates these profiles, they at least indicate the likely velocity structure of a significant proportion

Table 2. Least-squares fit parameters of the λ8037 CH_2CN^- models shown in Fig. 3. The mean LSR velocity (v_{LSR} / km s^{-1}), Doppler cloud width (b/km s^{-1}) and equivalent width of the model λ8037 DIB (W_{8037}/mÅ) are given along with the normalised continuum rms of the observed spectra (σ_c), and the rms of the model fit residuals (σ_f).

Sightline	v_{LSR}	b	W_{8037}	σ_c	σ_f
Cyg OB2 5	13.9	21.6	32.5	0.0020	0.0014
Cyg OB2 8a	12.3	21.0	30.2	0.0024	0.0016
Cyg OB2 12	9.4	24.0	38.3	0.0024	0.0013
HD 168112	29.9	26.4	24.5	0.0018	0.0021
HD 169034	13.6	33.0	38.7	0.0036	0.0024
HD 183143	25.0	18.0	37.5	0.0022	0.0012
HD 186745	19.3	16.2	24.3	0.0014	0.0013
HD 229196	14.1	21.6	22.0	0.0020	0.0012

of the neutral gas in these sightlines, aided by the fact that the stars are relatively distant (see Table 1). The peak of the calculated CH_2CN^- distribution generally lies within c. 10–15 km s^{-1} of the peak H I column density. It should be noted that the mean LSR velocities of the foreground clouds traced by K I are positive for each sightline, which can be explained as a result of Galactic rotation and observational bias in the Galactic longitude of the targets. In Fig. 4 there is an additional systematic small shift in the inferred CH_2CN^- distribution to a higher LSR velocity as compared to the K I. It is possible that this originates from the difficulty in defining the continuum of λ8037 as it sits atop a (variable) 8040 Å broader feature.

Analysis of the velocity structure of interstellar gas in the observed sightlines has been performed to determine whether the DIB profiles can be reproduced by convolving the transitions of CH_2CN^- with the observed interstellar gas distributions. The results of the least-squares fitting (Table 2) show that a Doppler b parameter of ~20 km s^{-1} is required to achieve a good fit with the DIB. Typically, clouds traced by K I are much narrower than this (Welty & Hobbs 2001), and even in heavily-reddened lines of sight such as those observed, the presence of multiple K I clouds separated in velocity space is insufficient to account for such broadening. Examining the data in left-hand panel of Fig. 4, the HD 183143 least-squares model CH_2CN^- distribution shows gross similarities with the Ti II and Ca II profiles. It is evident from these spectra that Ti II has a broader and less-peaked distribution than the other species. In order of decreasing profile width and increasing structure, Ti II comes first followed by Ca II, then CH^+, and finally K I. This sequence is believed to reflect the typical conditions in the clouds in which these species are generally found (see for example Jenkins 1989; Crinklaw et al. 1994; Welty 1998; Welty et al. 2003; Pan et al. 2005). Ti II, due to its high condensation temperature tends to be found in the gas phase in hotter, more heavily shocked higher velocity clouds, and is depleted out onto grains in cool, quiescent diffuse clouds and molecular clouds. Ca has a similar condensation temperature to Ti and therefore comes out of the solid state to produce Ca II in similar energetic/shocked regions to where Ti II is observed, but will be ionised to Ca III in more diffuse, strongly irradiated clouds, so it tends to be found in greatest abundances in warm yet moderately well-shielded regions. CH^+ is photodissociated in less dense regions, but has been shown to have a broader velocity distribution than K I (Pan et al. 2005), consistent with the formation of this molecule in warmer haloes surrounding cold cloud cores (Crawford et al. 1994). K I is a good tracer for cool, quiescent, well-shielded clouds with low thermal broadening where the radiation field is attenuated and the photoionisation rate is relatively low. Based on this information and

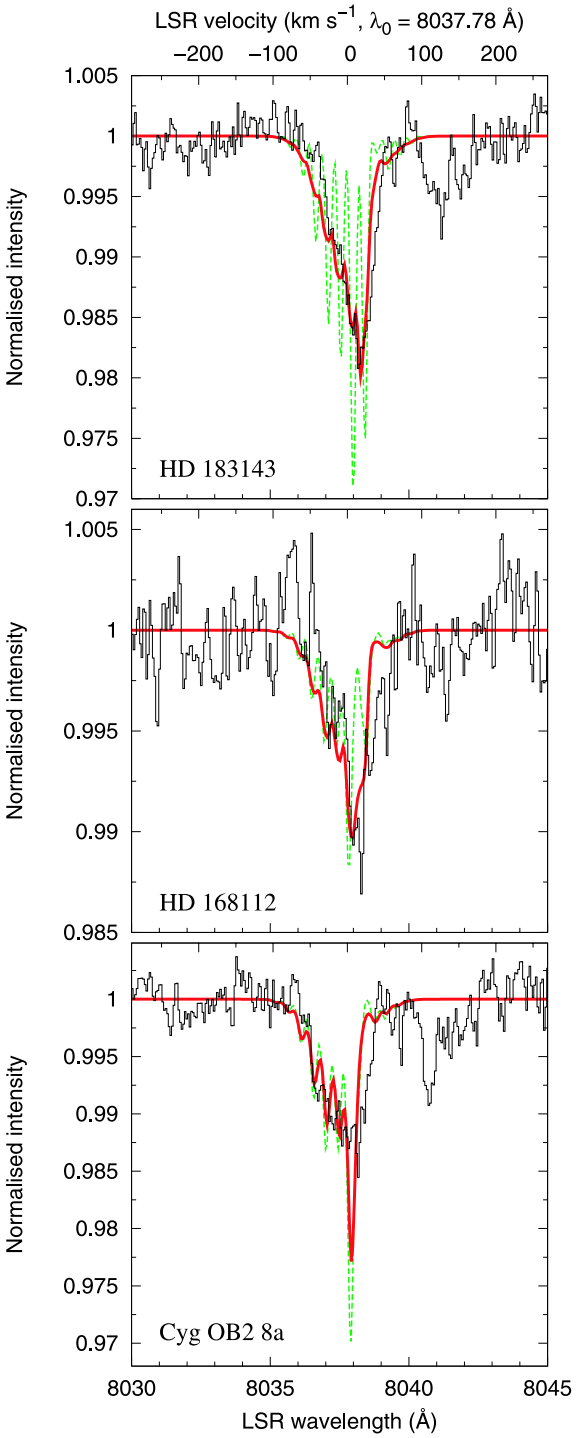

Fig. 5. 2.74 K CH_2CN^- $^1B_1 - \tilde{X}\ ^1A'$, $K_a'' = 0$ transitions convolved with the HIRES PSF and the interstellar Ti II profiles (solid lines), and the K I profiles (dashed lines), observed towards HD 183143, HD 168112 and Cyg OB2 8a, overlaid on the normalised, telluric-corrected λ8037 DIB profiles (thin black histograms).

the breadth of the Ti II distributions shown in Fig. 4, gas traced by Ti II may plausibly have a velocity distribution sufficient to provide the Doppler broadening required for CH_2CN^- to be the carrier of λ8037. Ti III and other gases present in regions where H II is found may exist over an even greater range of velocities.

Figure 5 shows the convolution of the 2.74 K CH_2CN^- $^1B_1 - \tilde{X}\ ^1A'$, $K_a'' = 0$ transitions with the (HIRES) instrumental PSF and with the interstellar Na I and Ti II profiles for each of the

three sightlines. Noiseless Na I and Ti II velocity profiles were derived by modelling the Na I UV doublet and the Ti II 3242 and 3384 Å lines using the VAPID routine (Howarth et al. 2002). The accuracy of the derived Doppler *b* parameters was improved by the simultaneous modelling of two transitions of each species (originating in the same ground state), with differing oscillator strengths. Due to its similar chemistry, Na I traces the same type of interstellar material as K I, and was used in preference to the K I 7699 Å lines shown in Fig. 4 due to the reduced saturation and telluric contamination of the Na I UV doublet. Atomic transition parameters were taken from Morton (2003).

Within the spectral signal-to-noise, the profiles in Fig. 5 calculated by convolution of the CH_2CN^- transitions with the interstellar Ti II profiles compare favourably with the diffuse interstellar band wavelength and profile, especially for HD 168112 and HD 183143. Convolution by Ti II gives a significantly better fit than convolution by Na I in all three cases, where the narrowness of the Na I Doppler spread produces structure in the resulting contour which is not seen in the observed DIB. These results demonstrate that the origin band CH_2CN^- $^1B_1 - \tilde{X}$ $^1A'$, $K_a = 1 \longleftarrow 0$ transitions at 2.74 K are capable of reproducing the narrow λ8037 DIB towards HD 183143 and HD 168112 provided that the postulated CH_2CN^- carrier molecule is distributed in velocity space in approximately the same way as interstellar Ti II. Due to the lack of substructure in the observed λ8037 profile, it is very unlikely that CH_2CN^- could instead coexist with Na I and K I in the cold neutral medium. For Cyg OB2 8a the peak absorption wavelength and profile match is reasonably good for the case of both Na I and Ti II, but there is clearly a significant level of structure in the calculated profiles that is not present in the observation. For the Ti II-convolved calculations, the relatively small differences between the calculated and observed profiles could plausibly be the result of Poisson noise of the spectrum or other features contaminating the DIB profile such as other interstellar features, telluric division or flat-fielding residuals.

6. Discussion

Under the assumption that the CH_2CN^- distribution is the same as that of Ti II – with the implication that CH_2CN^- co-exists with gas-phase Ti II – the fit to the observed λ8037 spectrum towards HD 183143 and HD 168112 is very good (and to a lesser degree for Cyg OB2 8a). This result leads to two possibilities for the type of gas with which the postulated CH_2CN^- might be most closely associated: (1) The warm, shocked "intercloud" medium; for the ~50 interstellar clouds expected to be present in the heavily-reddened sightlines studied (see Welty et al. 2003), the warm, low density, shocked clouds with low depletions should dominate the Ti II profiles (e.g. Crinklaw et al. 1994). (2) The neutral ISM; Ti II is a good tracer of neutral hydrogen due to its ionisation potential of 13.6 eV (Stokes 1978). Without knowledge of the precise H I velocity profiles, the possibility that the postulated CH_2CN^- co-exists with neutral atomic hydrogen gas cannot be ruled out.

There are no reports of past attempts to detect CH_2CN^- or CH_2CN in the diffuse ISM. The neutral radical CH_2CN has been observed in the dense TMC-1 and Sgr B2 molecular clouds (see Irvine et al. 1988; Turner et al. 1990) through its pure rotational transitions. Fractional abundances are $\sim 10^{-9}$ to 10^{-11} relative to H_2, and CH_2CN was found to be similarly distributed to CH_3CN and C_4H. The synthesis of CH_2CN in the shocked diffuse interstellar clouds traced by Ti II could be driven by the release of hydrocarbons into the gas phase during supernova shock-induced collisions between carbonaceous grains (Duley & Williams 1984; Hall & Williams 1995). Given a sufficient abundance of $C_2H_4^+$ in the gas phase, the reaction

$$C_2H_4^+ + N \longrightarrow CH_3CN^+ + H, \quad (1)$$

with a rate coefficient of $\sim 10^{-10}$ cm^3 s^{-1} (Herbst & Leung 1990), could proceed rapidly enough to produce sufficient quantities of CH_3CN^+ to allow dissociative recombination (DR)

$$CH_3CN^+ + e \longrightarrow CH_2CN + H \quad (2)$$

to occur. This mechanism for CH_2CN production is only viable if single H-atom loss is a significant channel in the DR of CH_3CN^+ (a process which is yet to be studied in detail), and if recombination occurs before CH_3CN^+ is destroyed by reacting with neutral hydrogen. The dominant mechanisms by which CH_2CN and CH_3CN are expected to be destroyed in the diffuse ISM are by photodissociation and by reaction with C^+.

The most obvious pathway for production of the cyanomethyl anion CH_2CN^- is by radiative electron attachment to CH_2CN:

$$CH_2CN + e \longrightarrow CH_2CN^- + h\nu, \quad (3)$$

though an alternative route exists via dissociative attachment to CH_3CN:

$$CH_3CN + e \longrightarrow CH_2CN^- + H. \quad (4)$$

The last step was studied by Sailer et al. (2003) in the laboratory. The dissociative electron attachment cross-section peaked at 4×10^{-23} m^2 for electron energies of 3.2 eV, which provides an efficient route to the formation of CH_2CN^- from CH_3CN. The cyanomethyl anion production channel is ~500 times more efficient than those of the other possible anionic fragments ($CHCN^-$, CCN^-, CN^- and CH_3^-) for electrons energies between 1 and 10 eV. In the interstellar context, photon and cosmic ray impact on grains could provide a source of electrons with a few eV energy.

If the dominant chemical reactions involving CH_2CN^- are assumed to be formation of the anion via radiative attachment (Eq. (3)) and destruction via photodetachment, then in equilibrium, the anion-to-neutral ratio is given by

$$\frac{[CH_2CN^-]}{[CH_2CN]} = \frac{\alpha n_e}{\Gamma} \quad (5)$$

where α is the rate of radiative electron attachment, n_e is the electron density and Γ is the photodetachment rate. Following s-wave electron capture by CH_2CN into an excited state of CH_2CN^- (Terzieva & Herbst 2000), if subsequent radiative relaxation occurs rapidly, either by vibrational transitions of the vibrationally excited ground state or by electronic transitions from the dipole-bound state to the ground state, then α can be estimated using Eq. (6) of Terzieva & Herbst (2000). In the diffuse ISM (at $T = 100$ K), this yields a value of $\alpha = 2.2 \times 10^{-7}$ cm^{-3} s^{-1}, assuming that the exited anion undergoes radiative stabilisation before the electron detaches back to the continuum. The photodetachment rate Γ has been calculated to be approximately 1.2×10^{-8} s^{-1} (E. Herbst & T. J. Millar, private communication) in the standard interstellar radiation field (Draine 1978). Both parameters are uncertain due to the lack of laboratory or theoretical data for this molecule, but nevertheless permit a rough estimate of the fraction of CH_2CN likely to occur in anionic form. Using an electron density in the diffuse ISM of

between 0.04 and 0.23 cm^{-3} (Welty et al. 2003), Eq. (5) yields an anion-to-neutral ratio between 0.7 and 4.2. If CH_2CN^- is present in the warm neutral medium traced by Ti II (and Ca II) where $T \sim 4000$ K (see Welty et al. 1996) then $\alpha = 3.4 \times 10^{-8}$ cm^{-3} s^{-1} and the calculated anion-to-neutral ratio is 0.1−0.7.

A further test of the plausibility of CH_2CN^- as carrier of the λ8037 DIB is whether a feasible CH_2CN abundance can be deduced from the equivalent width of the observed DIB. Polyatomic molecules are likely to be present in all of the heavily-reddened sightlines towards which λ8037 was observed. Cyg OB 12, Cyg OB2 5 and HD 183143 have been studied by McCall et al. (1998, 2002a), particularly with reference to interstellar H_3^+, detected in all three sightlines with Doppler $b \sim 10$ km s^{-1} which is substantially broader than the ^{13}CO and HCO^+ lines observed towards Cyg OB2 12. The HCO^+ column density was found to be $\sim 10^{11}$ cm^{-2}. Scappini et al. (2002) determined a likely total number density of $n \gtrsim 10^4$ cm^{-3} for the gas containing the CO and HCO^+, with the inference of dense, compact molecular clumps within a more diffuse medium. The approximate molecular hydrogen column density towards Cyg OB2 12 (from McCall et al. 2002a) is 6.5×10^{21} cm^{-2} such that the fractional HCO^+ abundance is $\sim 1.5 \times 10^{-11} n_{H_2}$.

The equivalent width of the λ8037 DIB is 38.3 mÅ (see Table 2) which requires a column density of $N(CH_2CN^-) = 6.7 \times 10^{10}$ cm^{-2}/f where f is the oscillator strength of the transition. Transitions between the ground and dipole-bound states are strongly observed in the lab (Lykke et al. 1987), suggesting that the value of f should be relatively large. Therefore, if $f = 0.5$ and assuming a CH_2CN anion-to-neutral ratio of 1, a molecular fraction of CH_2CN of $2 \times 10^{-11} n_{H_2}$ is required towards Cyg OB2 12 to produce the observed λ8037 equivalent width. Thus, provided the $^1B_1 - \tilde{X}\ ^1A'$ transition is strong, the required interstellar CH_2CN fractional column density is comparable to that of HCO^+ observed in the Cyg OB2 12 sightline. Averaged along the sightline, the required interstellar CH_2CN fractional abundance is at the lower end of the range of values found in dense molecular clouds ($\sim 10^{-11}$–$10^{-9} n_{H_2}$). If diffuse and dense cloud molecular abundances are similar, then enough CH_2CN^- can probably be produced to create the λ8037 DIB along heavily-reddened sightlines.

The spectra observed by McCall et al. (2002a) show clearly that the interstellar material traced by H_3^+ has a broader velocity distribution than the molecules (CO, C_2, CN) which typically trace dense molecular material. The H_3^+ line *FWHM* observed towards Cyg OB2 12, Cyg OB2 5 and HD 183143 range from 8 to 15 km s^{-1} whereas the CN line *FWHM* are all less than 4 km s^{-1}. McCall et al. (2002a) conclude that "the chemistry that leads to H_3^+ is completely decoupled from that which is responsible for these heavier diatomics". These factors lend support to the possibility that other molecules may be present in significant abundances in the more diffuse regions surrounding conventional molecular clouds.

Very rapid production mechanisms are required for molecules such as CH_2CN and its anion to exist in the warm diffuse regions traced by Ti II, though PAHs and related large organic species will survive for much longer in the UV radiation field with the potential to give rise to diffuse interstellar bands. The interstellar media containing Ti II and Ca II are largely cospatial (see Crinklaw et al. 1994; Albert et al. 1993), and these refractory ions are observed predominantly in the warm neutral ISM. Welty et al. (1996) found the mean upper temperature limit of the clouds in their Ca II survey to be 4100 K, though temperatures as low as a few hundred K were found in many cases. Titanium and calcium arise in the gas phase predominantly due to grain destruction (Stokes 1978), and it is plausible that molecules and DIB carriers may also arise in this way.

There is no evidence in the literature for correlations between DIB strengths and Ti II column densities, though Herbig (1993) found that the 5780 and 5797 DIBs do not correlate with the level of titanium depletion. This study suggests that further investigation of a possible link between DIBs, molecules and Ti II is warranted.

7. Conclusion

Using the rotational constants of Lykke et al. (1987), the absorption spectrum arising from the $^1B_1 - \tilde{X}\ ^1A'$ transition of CH_2CN^- has been computed for CH_2CN^- in equilibrium with the CMB at 2.74 K. The peak of the intrinsic absorption profile (at 8037.78 Å) is consistent with the peak of the diffuse interstellar absorption feature at 8037.8 ± 0.15 Å found in the spectra of eight heavily-reddened stars. If CH_2CN^- occurs in the ISM with the statistical ortho : para abundance ratio of 3:1 the $^1B_1 - \tilde{X}\ ^1A'$ transitions with $K_a'' = 1$ would produce strong spectral features at wavelengths of approximately 8024.8 and 8049.6 Å that are not present in the observed interstellar spectra. However, if the $K_a'' = 1$ level is populated based on a Boltzmann distribution at 2.74 K, then the $K_a = 0 \longleftarrow 1$ and $K_a = 2 \longleftarrow 1$ subbands are sufficiently weak to be compatible with their absence from the observed spectra. A thermal (Boltzmann) distribution of K_a'' levels would be expected if an efficient mechanism exists for conversion between the ortho and para forms of CH_2CN^-. Alternatively, the formation mechanism(s) for CH_2CN^- may introduce a skewed (i.e. non 3:1) ratio of ortho and para forms. Higher signal-to-noise ($\gtrsim$2000) spectroscopic observations of the λ8037 region will assist in the search for the $K_a'' = 1$ subbands. Without detailed laboratory or theoretical studies, it is unclear whether or not the CH_2CN^- formation mechanism(s) would result in the required deviation of the ortho-to-para ratio from the statistical value of 3:1.

The cyanomethyl anion CH_2CN^- is a plausible candidate for the carrier of the narrow diffuse interstellar band located at 8037.8 Å, provided a spectral line-broadening mechanism can be accounted for that produces an approximately Gaussian broadening corresponding to a Doppler b of between 16 and 33 km s^{-1} which corresponds with the observed Ti II and Ca II profiles towards HD 183143 and HD 168112, and is comparable to the H_3^+ linewidths towards Cyg OB2 12, Cyg OB2 5 and HD 183143.

Measurement of the oscillator strength of the $^1B_1 - \tilde{X}\ ^1A'$ transition would enable the calculation of the interstellar column density of CH_2CN^- that would be required to produce the λ8037 DIB. Assuming the transition is strong ($f \sim 0.5$), and the CH_2CN anion-to-neutral ratio is large (~1, as suggested by preliminary calculations of the anion formation and destruction rates), then towards Cyg OB2 12 the required average fractional abundance of neutral CH_2CN relative to H_2 is 2×10^{-11}, which falls at the lower end of the observed range in dense clouds.

The spectroscopic consistency between the λ8037 DIB and the calculated transitions of CH_2CN^- cannot be considered an assignment, but provides strong motivation for further study of this molecular anion including a search for the pure rotational transitions of interstellar CH_2CN^-.

Acknowledgements. The authors would like to thank George Herbig for kindly making available extensive Keck HIRES data and Ian Howarth for providing the VAPID software and support. MAC thanks EPSRC for a studentship and the

University of Nottingham for financial support. We also thank Tom Millar and Steve Fossey for helpful comments, and a referee for suggested improvements to the manuscript. This research has made use of the SIMBAD database, operated at CDS, Strasbourg, France. The W. M. Keck Observatory is operated as a scientific partnership among the California Institute of Technology, the University of California, and NASA. The observatory was made possible by the generous financial support of the W. M. Keck Foundation.

References

Albert, C. E., Blades, J. C., Morton, D. C., et al. 1993, ApJS, 88, 81
Birss, F. W., & Ramsay, D. A. 1984, Comp. Phy. Commun., 38, 83
Brinkman, E. A., Berger, S., Marks, J., & Brauman, J. I. 1995, J. Chem. Phys., 99, 7586
Compton, R. N., Carman, H. S., Desfrançois, C., Abdoul-Carime, H., & Scherman, J. P. 1996, J. Chem. Phys., 105, 6126
Crawford, I. A., Barlow, M. J., Diego, F., & Spyromilio, J. 1994, MNRAS, 266, 903
Crawford, O. H. 1970, Mol. Phys., 20, 585
Crinklaw, G., Federman, S. R., & Joseph, C. L. 1994, ApJ, 424, 748
Dalgarno, A., & McCray, R. A. 1973, ApJ, 181, 95
Desfrançois, C., Abdoul-Carime, H., & Scherman, J. P. 1996, Int. J. Mod. Phys., 10, 1339
Dickens, J. E., & Irvine, W. M. 1999, ApJ, 518, 733
Draine, B. T. 1978, ApJS, 36, 595
Duley, W. W., & Williams, D. A. 1984, MNRAS, 211, 97
Fermi, E., & Teller, E. 1947, Phys. Rev., 72, 406
Flower, D. R., & Watt, G. D. 1984, MNRAS, 209, 25
Güthe, F., Tulej, M., Pachkov, M. V., & Maier, J. P. 2001, ApJ, 555, 466
Galazutdinov, G. A., Krełowski, J., & Musaev, F. A. 1999, MNRAS, 310, 1017
Galazutdinov, G. A., Musaev, F. A., Krełowski, J., & Walker, G. A. H. 2000, PASP, 112, 648
Garrett, W. R. 1978, J. Chem. Phys., 69, 2621
Gredel, R., & Munch, G. 1994, AA, 285, 640
Gutsev, G. L., & Adamowicz, L. 1995a, Chem. Phys. Lett., 246, 245
Gutsev, G. L., & Adamowicz, L. 1995b, J. Phys. Chem., 99, 13412
Gutsev, G. L., & Adamowicz, L. 1995c, Chem. Phys. Lett., 235, 377
Hall, P., & Williams, D. A. 1995, Ap&SS, 229, 49
Herbig, G. H. 1993, ApJ, 407, 142
Herbig, G. H. 1995, Annu. Rev. Astophys., 33, 19
Herbig, G. H., & Leka, K. D. 1991, ApJ, 382, 193
Herbst, E. 1981, Nature, 289, 656
Herbst, E., & Leung, C. M. 1990, A&A, 233, 177
Herbst, E., & Petrie, S. 1997, ApJ, 491, 210
Howarth, I. D., Price, R. J., Crawford, I. A., & Hawkins, I. 2002, MNRAS, 335, 267
Irvine, W. M., Friberg, P., Hjalmarson, A., et al. 1988, ApJ, 334, L107
Jenkins, E. 1989, in Interstellar Dust, IAU Symp. 135, 23
Kalberla, P. M. W., Burton, W. B., Hartmann, D., et al. 2005, VizieR Online Data Catalog, 8076, 0
Lakin, N. M., Pachkov, M., Tulej, M., et al. 2000, J. Chem. Phys., 113, 9586
Le Teuff, Y. H., Millar, T. J., & Markwick, A. J. 2000, A&AS, 146, 157
Liszt, H., & Lucas, R. 2001, A&A, 370, 576
Lucas, R., & Liszt, H. 1996a, A&A, 307, 237
Lucas, R., & Liszt, H. S. 1996b, in Molecules in Astrophysics: Probes & Processes, IAU Symp., 178, 421
Lucas, R., & Liszt, H. S. 2000, A&A, 358, 1069
Lykke, K. R., Neumark, D. M., Andersen, T., Trapa, V. J., & Lineberger, W. C. 1987, J. Chem. Phys., 87, 6842
Maier, J. P., Lakin, N. M., Walker, G. A. H., & Bohlender, D. A. 2001, ApJ, 553, 267
Massey, P., & Thompson, A. B. 1991, AJ, 101, 1408
McCall, B. J., Geballe, T. R., Hinkle, K. H., & Oka, T. 1998, Science, 279, 1910
McCall, B. J., Thorburn, J., Hobbs, L. M., Oka, T., & York, D. G. 2001, ApJ, 559, L49
McCall, B. J., Hinkle, K. H., Geballe, T. R., et al. 2002a, ApJ, 567, 391
McCall, B. J., Oka, T., Thorburn, J., Hobbs, L. M., & York, D. G. 2002b, ApJ, 567, L145
McCarthy, M. C., Gottlieb, C. A., Gupta, H., & Thaddeus, P. 2006, ApJ, 652, L141
Millar, T. J., Herbst, E., & Bettens, R. P. A. 2000, MNRAS, 316, 195
Millen, D. J., Topping, G., & Lide, D. R. J. 1962, J. Molo. Spec., 8, 153
Moran, S., Ellis, B. J., Defrees, D. J., Mclean, A. D., & Ellison, G. B. 1987, J. Am. Chem. Soc., 109, 5996
Morton, D. C. 2003, ApJS, 149, 205
Ozeki, H., Hirao, T., Saito, S., & Yamamoto, S. 2004, ApJ, 617, 680
Pan, K., Federman, S. R., Sheffer, Y., & Andersson, B.-G. 2005, ApJ, 633, 986
Perryman, M. A. C., & ESA. 1997, The HIPPARCOS and TYCHO catalogues. Astrometric and photometric star catalogues derived from the ESA HIPPARCOS Space Astrometry Mission (Noordwijk, The Netherlands: ESA Publications Division), ESA SP Ser., 1200
Ruffle, D. P., Bettens, R. P. A., Terzieva, R., & Herbst, E. 1999, ApJ, 523, 678
Sailer, W., Pelc, W., Limao-Vieira, P., et al. 2003, Chem. Phys. Lett., 381, 216
Sarre, P. J. 1980, J. Chim. Phys., 77, 769
Sarre, P. J. 2000, MNRAS, 313, L14
Sarre, P. J. 2006, J. Mol. Spec., 238, 1
Sarre, P. J., & Kendall, T. R. 2000, in Astrochemistry: from Molecular Clouds to Planetary Systems, IAU Symp., 197, 343
Savage, B. D., & Sembach, K. R. 1991, ApJ, 379, 245
Scappini, F., Casu, S., Cecchi-Pestellini, C., & Olberg, M. 2002, MNRAS, 337, 495
Sommerfeld, T. 2005, J. Phys.: Conf. Ser., 4, 245
Stokes, G. M. 1978, ApJS, 36, 115
Takakuwa, S., Kawaguchi, K., Mikami, H., & Saito, M. 2001, PASJ, 53, 251
Terzieva, R., & Herbst, E. 2000, Int. J. Mass Spectrom., 201, 135
Tulej, M., Kirkwood, D. A., Pachkov, M., & Maier, J. P. 1998, ApJ, 506, L69
Turner, B. E., Friberg, P., Irvine, W. M., Saito, S., & Yamamoto, S. 1990, ApJ, 355, 546
Tyler, J., Sheridan, J., & Costain, C. C. 1972, J. Mol. Spectrosc., 43, 248
van Dishoeck, E. F., & Black, J. H. 1986, ApJS, 62, 109
Wegner, W. 1994, MNRAS, 270, 229
Wegner, W. 2006, MNRAS, 371, 185
Welty, D. 1998, IAU Colloq. 166, The Local Bubble and Beyond, LNP, 506, 151
Welty, D. E., & Hobbs, L. M. 2001, ApJS, 133, 345
Welty, D. E., Morton, D. C., & Hobbs, L. M. 1996, ApJS, 106, 533
Welty, D. E., Hobbs, L. M., & Morton, D. C. 2003, ApJS, 147, 61